

Original Article

An AC-DC Interleaved ZCS-PWM Boost Converter with Reduced Auxiliary for High-Voltage EV Battery Systems

A.Mathavan¹, K.Gokulraj²

^{1,2}E.G.S Pillay Engineering College Nagapattinam, Tamilnadu, India.

Received Date: 27 April 2023

Revised Date: 08 May 2023

Accepted Date: 10 May 2023

Abstract: This work presents a novel approach for the design of a single-stage AC/DC isolated adaptive-network-based fuzzy inference system (ANFIS) controller for board chargers in electric vehicles (EVs) with high-voltage (HV) battery systems. The proposed converter utilizes a modular stacked switches structure with interleaved control, combining modular interleaved bridgeless AC/DC boost converters and modular CLL resonant circuits. By sharing the two legs of the stacked switches, the voltage stress across each switch is reduced to half of the DC-link voltage, making it suitable for HV battery systems (e.g., 800 V) in EVs.

The design incorporates integrated interleaved boost circuit modules to achieve low input current ripple. Two step-up resonant circuit modules are connected to the interleaved legs, with their outputs connected in series at the input of a current-fed high-frequency rectifier. To achieve soft-switching commutation, an ANFIS is used for all switches and diodes in the proposed converter.

The performance of the proposed design was validated through simulations using MATLAB Simulink. The results demonstrated that the converter achieved a peak efficiency, confirming its effectiveness in charging HV battery systems in EVs.

Keywords: EV Battery System, AC/DC Converter, ZCS-PWM Boost Converter.

I. INTRODUCTION

The significant advancements in Internal Combustion Engine (ICE) vehicles, powered by diesel or petrol, have contributed to a global increase in air pollution. To mitigate CO₂ emissions, numerous countries are actively researching electric vehicles (EVs) as an alternative. In addition to fossil fuel depletion, the need for alternative power sources for transportation has become crucial. The Indian government has set ambitious targets in the field of electric vehicles, aiming to replace all three-wheeler diesel/petrol vehicles with EVs by 2030. They also plan to achieve a 35% sales share for electric cars, 75% for commercial cars, 45% for public transport, and 75% for auto-rickshaws and bikes.

The propulsion and fuel source of an electric vehicle are of utmost importance. Electric cars are powered by electric current, leading to inquiries about the charging methods. Fast charging, also known as DC charging, involves the use of a DC charging station that converts alternating current (AC) to direct current (DC). By bypassing the on-board charger, the DC power is sent through the Battery Management System (BMS) and directed to the battery as instructed by the vehicle's charging control system.

Given the presence of both AC and DC currents, there are two main strategies for charging electric cars. AC charging stations rely on the on-board charger for the conversion process. Although this method is slower, it is cost-effective and less demanding. AC chargers typically have an output of up to 22 kW, and the time required for a full charge depends on the capacity of the on-board charger.

On the other hand, DC charging stations offer faster charging times, albeit at a higher cost. These stations provide direct current at an output of 50 kW, with the expectation of increasing in the future. Rapid chargers, with a power of 150 kW, are also available and are typically situated along major routes, intended for longer journeys.



To further complicate matters, there are various types of charging connectors in use. However, international standards and adapters are being developed, reducing the potential issue of compatibility in the future, similar to the adoption of standardized electrical sockets worldwide.

II. SURVEY

Mishima et al. proposed a single-stage high frequency-link soft-switching three-phase AC-DC converter for EV battery chargers. The converter utilizes a boost full-bridge (BFB) topology-based phase module to convert three-phase utility frequency AC (UFAC) to single-phase high-frequency AC (HFAC) without the need for a smoothed DC link. This design offers simplicity, cost-effectiveness, modularity, and high efficiency in power supply.

Kouski et al. introduced a single-stage AC-DC converter for bi-directional EV battery chargers. The converter utilizes a HB-FB resonant converter with back-to-back MOSFETs on its AC half-bridge. A proper controller is proposed to enable operation with a wide range of active and reactive power, as well as input and output voltage. The controller facilitates Zero Voltage Switching (ZVS) for all switching instants, minimizing conduction losses.

Kim et al. presented a single-stage AC/DC resonant converter for wireless power transfer in EVs. The converter integrates a power factor correction (PFC) converter and a three-level resonant converter into one. It operates at a fixed frequency and provides a wide controllable output voltage range (200Vdc to 400Vdc) with high efficiencies across a broad load range due to phase shift control.

Luca et al. proposed a modulation strategy for the 25 kW AC-DC isolated Matrix Charger three-phase rectifier (MCharger). The Matrix Charger topology allows for current and voltage regulation in EV energy storage devices. Compared to a standard Dual-Active-Bridge topology, the Matrix converter performs AC-AC energy conversion directly, eliminating the need for a rectifying stage.

Koushki et al. presented an isolated, single-stage bi-directional AC-DC converter for EV battery chargers. This converter, which features no electrolytic capacitor and 8 active switches, prevents low-frequency power ripple from reaching the battery. This prevents excess heat generation in the battery, resulting in increased battery longevity.

Saran et al. proposed a home charging system for electric rickshaws with a two-stage power conversion process. The system includes an AC-DC power conversion stage using a modified Cuk converter based on Vienna rectification. It maintains power quality according to international standards and keeps a constant DC-link despite variations in AC power supply. The primary stage output is fed to a split DC-link, and the second stage employs a half-bridge isolated converter with passive rectification on the secondary side.

Pandla Chinna et al. proposed a bidirectional AC/DC converter that combines an ac-dc grid bidirectional converter (GBC) with a dc-dc bidirectional battery charger (BBC). The GBC facilitates bidirectional power flow between the AC and DC grid, while the BBC enables bidirectional power flow between the energy storage system/EVs and the DC grid with isolation. A robust current control technique is employed for injecting power into the grid.

Rahman et al. investigated a single-stage bridgeless AC-DC charger for EVs with improved efficiency and revamped supply-side performance. The charger utilizes a conventional buck-boost DC-DC converter with positive voltage polarity at the output, addressing a major drawback of traditional converters. It also incorporates isolation and discontinuous inductor current conduction mode (DICCM) of the transformer magnetizing inductance for enhanced safety features.

Jitendra et al. presented a need-based distributed coordination strategy (NDCS) for multiple EV storages in an islanded commercial hybrid AC/DC microgrid. The interlinking converter's control capacity is enhanced by incorporating combined power-droop and voltage-droop strategies, allowing regulation of the AC bus voltage by solely adjusting the DC bus voltage without affecting power-sharing capabilities.

Kumar et al. designed, controlled, and simulated a bidirectional on-board charger for battery electric vehicles (BEVs) with vehicle-to-grid (V2G) power transfer ability and reactive power support to the grid. The charger utilizes a three-phase AC-DC matrix converter topology for a single-stage on-board charging application. Direct power control (DPC) and space vector modulation (SVM) techniques are employed for charging current and reactive power flow control.

Das et al. presented a DAB-based three-phase AC-DC isolated converter with a novel modulation strategy. This converter achieves single-stage power conversion without the need for electrolytic capacitors, improving reliability and power density. It also incorporates open-loop power factor correction, soft switching of all semiconductor devices, and a simple linear relationship between the control variable and transferred active power. The proposed operation is thoroughly analyzed, with simulation results and experimental verification provided.

Shuguang et al. introduced a charging module utilizing interleaved parallel LLC resonant converter topology. The design and control strategy of the charging module are explained, along with a detailed description of the working principle of the interleaved parallel LLC resonant converter. A 20 kW prototype is developed based on this design.

Debashish et al. presented a double integral sliding mode control (DSMC) and variable phase-shift algorithm for a bi-directional EV charger based on a front-end bridgeless converter. An interleaved phase-shifted bridgeless converter is preferred for AC-DC bi-directional power conversion due to reduced switching losses and decreased passive filter components. The proposed control strategy addresses the complexity of achieving zero voltage switching during phase-reversal in the presence of grid distortion.

III. PROPOSED SYSTEM

This work proposes a novel single-stage AC/DC isolated adaptive-network-based fuzzy inference system (ANFIS) controller for high-voltage (HV) battery systems in electric vehicles (EVs). The converter utilizes a modular stacked switches structure and interleaved control to integrate modular interleaved bridgeless AC/DC boost converters with modular CLL resonant circuits. This configuration reduces the voltage stress across each switch to half of the DC-link voltage, making it suitable for HV battery systems in EVs, such as 800V. The integrated interleaved boost circuit modules enable low input current ripple. Two step-up resonant circuit modules are connected to the interleaved legs, with their outputs connected in series at the input of a current-fed high-frequency rectifier. The proposed converter achieves soft-switching commutation for all switches and diodes.

A. Description and Analysis of the Proposed Converter

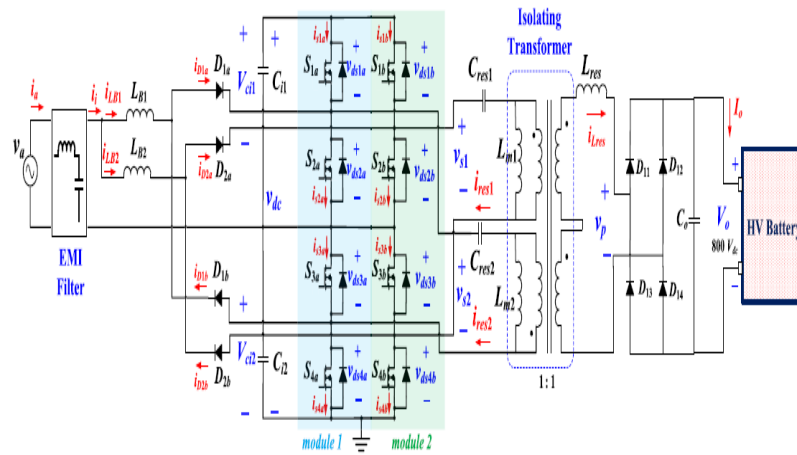


Figure 2: Proposed Interleaved Single-Stage AC/DC Converter with Modular Stacked Switches Configuration and Its Control Scheme

Figure 2 illustrates the proposed single-stage AC/DC high-gain converter designed for HV battery systems in electric vehicles (EVs). The converter consists of two interleaved modules, with each module comprising a bridgeless AC/DC boost converter integrated with a CLL resonant inverter through a stacked switches configuration (S1a-S4a and S1b-S4b). The outputs of the two resonant circuit modules are connected in series at the input of a current-fed high-frequency rectifier, which includes an input inductor (L_{res}).

By adopting the interleaved approach, both modules (1 and 2) in Figure 2 operate at the same switching frequency but are phase-shifted by 180° . In each leg of the stacked switches inverter (e.g., module 1), switches S2a and S3a have the

same duty ratio (d), while switches S_{1a} and S_{4a} operate with a duty ratio of $1-d$. Switches S_{1b} - S_{4b} follow the same control principle but are 180° phase-shifted from the switches in module 1. This configuration ensures that the voltage stress across each switch is reduced to half of the DC-link voltage (v_{dc}).

Each resonant circuit module consists of a resonant inductor (L_{res}), a high-frequency transformer magnetizing inductance (L_{m1} or L_{m2}), and a resonant capacitor (C_{res1} or C_{res2}). As the legs of the stacked switches are shared between the resonant converter stage and the input bridgeless AC/DC stage, each switch current comprises the resonant current (i_{res1} or i_{res2}) and the bridgeless boost power factor correction (PFC) inductor current (i_{LB1} or i_{LB2}). All switches in the interleaved modules are designed to achieve zero-voltage switching (ZVS) turn-on and zero-current switching (ZCS) turn-off.

The operating principles of the proposed converter for the two interleaved modules (a, b) are identical. Therefore, only the operating waveforms for module a are presented. During steady-state operation in the positive and negative half-cycles, the switching period (T_s) is divided into seven operating modes. Since the converter operates symmetrically during both positive and negative half-cycles, this analysis focuses on the positive half-cycle.

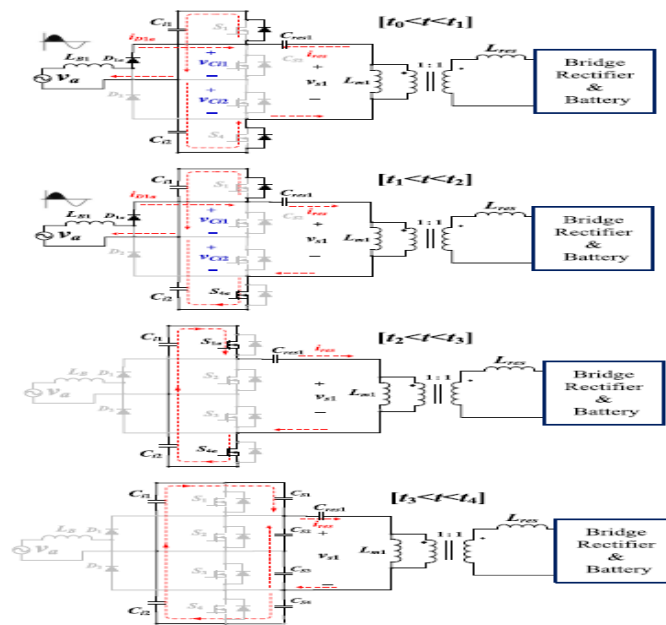


Figure 2: Operating Stages of One Module of the Proposed Converter within a Switching Period

The proposed converter operates in different stages within a switching period. Let's go through each stage:

During the stage $[t_0 < t < t_1]$, the boost inductor current is discharged through D_{1a} . When the gate signals are applied to S_{1a} and S_{4a} at time t_0 , the combined currents i_{res} and i_{D1a} cause the antiparallel diodes of S_{1a} to conduct. Similarly, the antiparallel diodes of S_{4a} also conduct due to the lagging resonant current i_{res} . In this stage, the voltage across switches S_{2a} and S_{3a} is clamped to half of the dc-link voltage ($v_{dc}/2$). The current flowing through switches S_{1a} and S_{4a} is a combination of the PFC inductor current and the resonant current, depending on the input source's positive or negative half-cycle.

In the stage $[t_1 < t < t_2]$, the switch S_{4a} changes polarity and turns on with zero-voltage switching (ZVS), while the antiparallel diode of S_{1a} remains on. At this point, the inductor current stops flowing through S_{4a} , indicating that the switch current is equal to the resonant current. The voltage across switches S_{2a} and S_{3a} remains clamped to half of the dc-link voltage.

During the stage $[t_2 < t < t_3]$, as the boost converter operates in discontinuous conduction mode (DCM), the current i_{D1a} becomes zero at $t = t_2$. The switch S_{1a} changes polarity, and the current previously flowing through the antiparallel diode is now conducted by S_{1a} , achieving ZVS. Similar to the previous stage, once the current polarity changes, the inductor current stops flowing through the switch, and the current through the switch becomes the resonant current.

In the stage $[t_3 < t < t_4]$, the gate signals v_{gs1a} and v_{gs4a} are removed, and the parasitic capacitances C_{s1} and C_{s4} of the MOSFETs start charging. As C_{s1} and C_{s4} are already discharged to the resonant circuit before this interval, the voltages across switches S_{1a} and S_{4a} (v_{ds1a} and v_{ds4a}) gradually start charging. This results in near-zero current turn-off for S_{1a} and S_{4a} . At the same time, C_{s2} and C_{s3} are discharged into the resonant circuit.

In the stage $[t_4 < t < t_5]$, at $t = t_4$, the boost inductor i_{D1a} begins to charge from zero, achieving zero-current turn-on for diode D_{1a} . At $t = t_4$, the difference between the resonant current and the D_{1a} current ($i_{res} - i_{D1a}$) causes the antiparallel diode of switch S_{2a} to conduct. Simultaneously, i_{res} forces the antiparallel diode of switch S_{3a} to conduct. The voltages across switches S_{2a} and S_{3a} during this interval are clamped to half of the dc-link voltage ($v_{dcl}/2$). The current flowing through the antiparallel diodes of the two switches varies based on the operating mode of the input ac voltage, with S_{2a} carrying a combination of the inductor and resonant current during the positive half-cycle and S_{3a} during the negative half-cycle.

In the stage $[t_5 < t < t_6]$, at $t = t_5$, the current flowing through the antiparallel diodes of S_{3a} and S_{2a} becomes zero, leading to ZVS turn-on for S_{2a} and S_{3a} .

B. Adaptive Network based Fuzzy Inference System (ANFIS)

The adaptive network based fuzzy inference system (ANFIS) is a data driven procedure representing a neural network approach for the solution of function approximation problems. Data driven procedures for the synthesis of ANFIS networks are typically based on clustering a training set of numerical samples of the unknown function to be approximated. Since introduction, ANFIS networks have been successfully applied to classification tasks, rule-based process control, pattern recognition and similar problems. Here a fuzzy inference system comprises of the fuzzy model proposed by Takagi, Sugeno and Kang to formalize a systematic approach to generate fuzzy rules from an input output data set.

ANFIS structure For simplicity, it is assumed that the fuzzy inference system under consideration has two inputs and one output. The rule base contains the fuzzy if-then rules of Takagi and Sugeno’s type as follows:

If x is A and y is B then z is $f(x,y)$ where A and B are the fuzzy sets in the antecedents and $z = f(x, y)$ is a crisp function in the consequent. Usually $f(x, y)$ is a polynomial for the input variables x and y . But it can also be any other function that can approximately describe the output of the system within the fuzzy region as specified by the antecedent. When $f(x,y)$ is a constant, a zero order Sugeno fuzzy model is formed which may be considered to be a special case of Mamdani fuzzy inference system [144] where each rule consequent is specified by a fuzzy singleton. If $f(x,y)$ is taken to be a first order polynomial a first order Sugeno fuzzy model is formed. For a first order two rule Sugeno fuzzy inference system, the two rules may be stated as: Rule 1: If x is A_1 and y is B_1 then $f_1 = p_1x + q_1y + r_1$ Rule 2: If x is A_2 and y is B_2 then $f_2 = p_2x + q_2y + r_2$ Here type-3 fuzzy inference system proposed by Takagi and Sugeno is used. In this inference system the output of each rule is a linear combination of the input variables added by a constant term. The final output is the weighted average of each rule’s output. The corresponding equivalent ANFIS structure is shown in Figure 3.

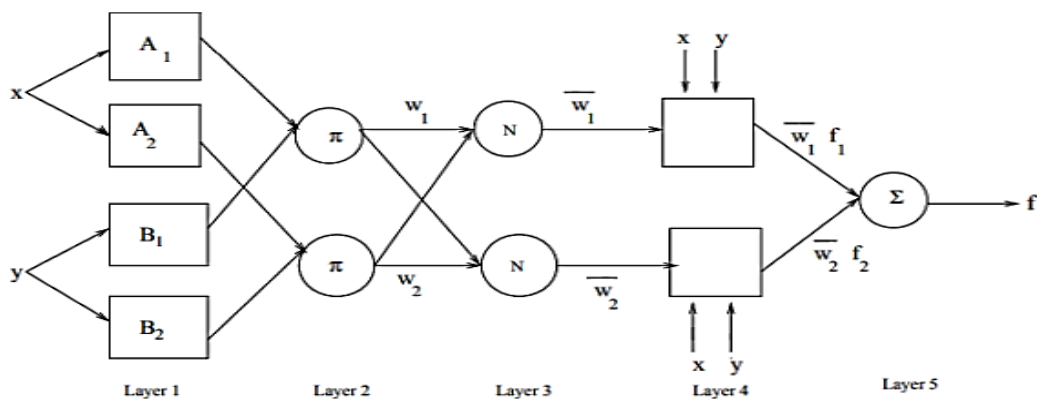


Figure 3: Type-3 ANFIS Structure

The derivation of the initial fuzzy model in an ANFIS-based system modeling follows a two-step process, as proposed by S.L. Chiu, which combines a cluster estimation method with a least squares estimation algorithm:

- In the first step, an initial fuzzy model is extracted from the input-output data using a cluster estimation method that considers all possible input variables. This method aims to identify the appropriate fuzzy rules and their associated premise parameters based on the available data. By clustering the data points, the algorithm determines the fuzzy membership functions and the corresponding rule parameters.
- In the second step, the important input variables are identified by testing the significance of each variable in the initial fuzzy model. This step involves evaluating the impact of each input variable on the overall model performance. By assessing the statistical significance of each variable's contribution to the model, the algorithm determines which variables are most relevant and should be included in the final fuzzy model.

Overall, this approach enables the construction of an optimal fuzzy model by iteratively refining the initial model based on the significance of each input variable. By selecting the important variables and optimizing the fuzzy rules, the method ensures that the resulting model accurately captures the relationships between the input and output data.

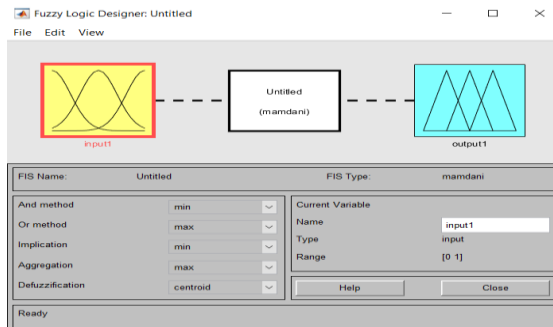


Figure 4: ANFIS model

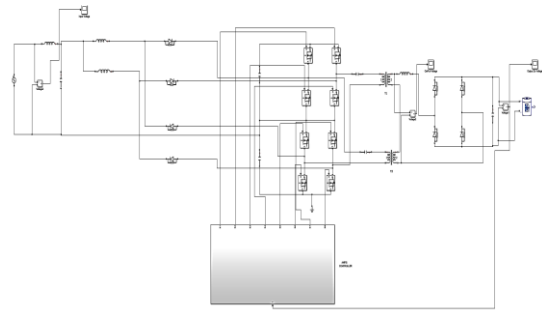


Figure 5: Over all Simulink model

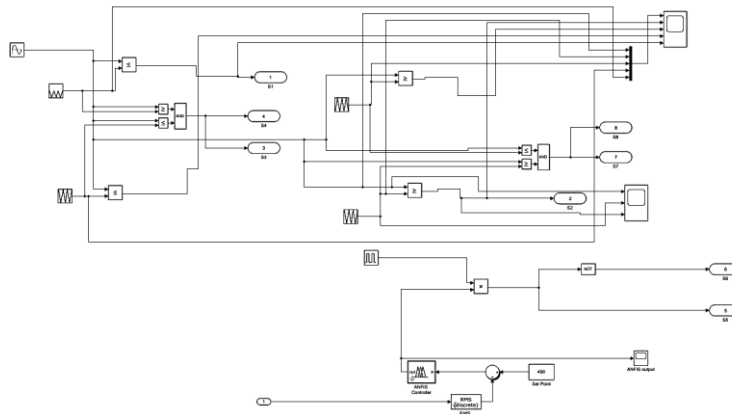


Figure 6: Control System

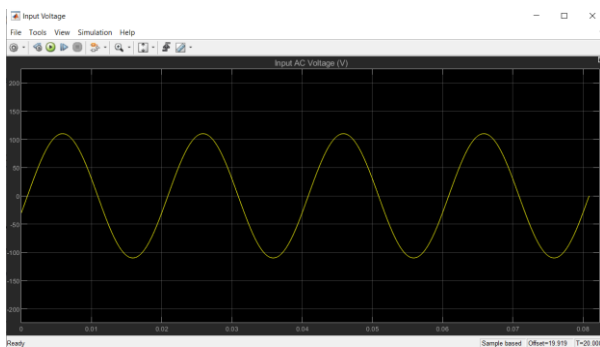


Figure 7: Input AC voltage



Figure 8: Output DC Voltage

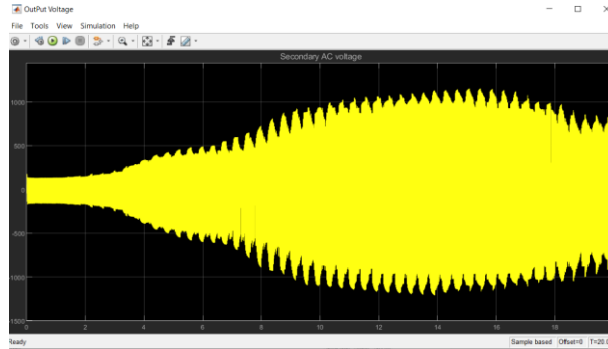


Figure 9: Output AC voltage

IV. CONCLUSION

This study introduces a novel ANFIS controlled single-stage ac/dc bridgeless step-up converter for HV battery on-board charger (OBC) systems in electric vehicle (EV) applications. The proposed circuit incorporates an integrated bridgeless boost rectifier with interleaved modules, connected in series with CLL resonant circuit modules and a current-fed output rectifier. This configuration allows for achieving the required high voltage (HV) gain necessary for HV battery systems. The paper provides a detailed description of the proposed ac/dc converter, including its operating principles and circuit characteristics. The circuit's ability to efficiently boost and regulate the voltage for HV battery systems is highlighted. The authors also present experimental results to validate and demonstrate the performance of the proposed topology.

Through these experimental results, the study provides evidence of the effectiveness and practical viability of the proposed converter. The findings support the claim that the proposed circuit design is a promising solution for HV battery OBC systems in EV applications, offering improved efficiency and performance compared to traditional converter topologies.

V. REFERENCES

- [1] Debasish Mishra;Bhim Singh;Bijaya Ketan Panigrahi; (2021). Adaptive Current Control for a Bidirectional Interleaved EV Charger With Disturbance Rejection. *IEEE Transactions on Industry Applications*.
- [2] Shuguang, LIU; Zhenxing, YE; Gang, CHENG (2019). [IEEE 2019 Chinese Control And Decision Conference (CCDC) - Nanchang, China (2019.6.3-2019.6.5)] 2019 Chinese Control And Decision Conference (CCDC) - Design and Realization of High Power Density EV Charging Module. , ()
- [3] Kumar, R., & Singh, B. (2020). Matrix Converter Based Single Stage Bidirectional On-Board EV Charger with Reactive Power Support. 2020 IEEE International Conference on Power Electronics, Smart Grid and Renewable Energy (PESGRE2020).
- [4] Das, Dibakar; Weise, Nathan; Basu, Kaushik; Baranwal, Rohit; Mohan, Ned (2018). A Bidirectional Soft-switched DAB based Single Stage Three Phase AC-DC Converter for V2G Application. *IEEE Transactions on Transportation Electrification*, (), 1-1.
- [5] Rahman, Md Shamiur; Hossain, Jahangir; Lu, Junwei; Pota, Hemanshu Roy (2017). A Need-Based Distributed Coordination Strategy for EV Storages in a Commercial Hybrid AC/DC Microgrid with an Improved Interlinking Converter Control Topology. *IEEE Transactions on Energy Conversion*, (), 1-1. doi:10.1109/TEC.2017.2784831
- [6] Saran Chaurasiya;Bhim Singh; (2020). A Home Charging System for EVs Using Vienna Based Modified Cuk Converter and LLC Resonant Converter . 2020 International Conference on Power, Instrumentation, Control and Computing (PICC), (), -.
- [7] Luca Rovere;Sabino Pipolo;Andrea Formentini;Pericle Zanchetta; (2020). AC-DC Isolated Matrix Converter Charger: Topology and Modulation . 2020 IEEE Energy Conversion Congress and Exposition (ECCE), (), -.
- [8] Mishima, Tomokazu; Mitsui, Shoya (2019). 2019 IEEE Energy Conversion Congress and Exposition (ECCE) - A Single-Stage High Frequency-link Modular Three-Phase Soft-Switching AC-DC Converter for EV Battery Charger., 2141-2147.
- [9] Kouski, Behnam; Jain, Praveen; Bakhshai, Alireza (2017). 2017 IEEE Applied Power Electronics Conference and Exposition (APEC) - Half-bridge full-bridge AC-DC resonant converter for bi-directional EV charger. , (), 3681-3687.
- [10] Kim, Minji; Marius, Takongmo; Lee, Gangwoo; Oh, Jaesung; Yoo, Kyungjong; Kim, Eunsoo; Hwang, Ingab (2019). [IEEE 2019 IEEE Applied Power Electronics Conference and Exposition (APEC) - Anaheim, CA, USA (2019.3.17-2019.3.21)] 2019 IEEE Applied Power Electronics Conference and Exposition (APEC) - A Single-Stage Three-Level AC/DC Converter for Wireless Power Transfer. ,f 3123-3128.
- [11] Koushki, Behnam; Jain, Praveen; Bakhshai, Alireza (2018). [IEEE 2018 IEEE Applied Power Electronics Conference and Exposition (APEC) - San Antonio, TX, USA (2018.3.4-2018.3.8)] 2018 IEEE Applied Power Electronics Conference and Exposition (APEC) - A single-stage bi-directional AC-DC converter with no electrolytic capacitor for EV. 1447-1454.
- [12] Jitendra Gupta;Bhim Singh; (2020). A Single Phase Pre-Regulated High Power-Factor Bridgeless Isolated AC-DC Converter for EV Charging Application . 2020 IEEE 7th Uttar Pradesh Section International Conference on Electrical, Electronics and Computer Engineering (UPCON).